Available online at www.sciencedirect.com
ScienceDirect
Journal of the European Ceramic Society 30 (2010) 525–530
www.elsevier.com/locate/jeurceramsoc

Grain growth behaviour of ZnO-based multilayer varistors

Shu-Ting Kuo, Wei-Hsing Tuan *

Department of Materials Science and Engineering, National Taiwan University, Taipei 106, Taiwan

Available online 31 May 2009

Abstract

In the present study, a model multilayer structure composing of seven Bi_2O_3-doped ZnO layers and AgPd inner electrodes is prepared. The Bi_2O_3-doped ZnO bulk specimens are also prepared for comparison purpose. The size of ZnO grains in the multilayer specimens is smaller than that in the bulk specimen. Furthermore, the size of ZnO grains in the multilayer specimens decreases with the decrease of layer thickness. Microstructure analysis demonstrates that the Bi_2O_3-rich liquid phase wets not only the ZnO grains but also the AgPd electrodes.

Keywords: ZnO; Varistor; Microstructure-final; Firing; Multilayer

1. Introduction

Due to the unique nonlinear *I–V* characteristics of ZnO–Bi_2O_3-based ceramics, they are applied as varistors to protect electronic devices against voltage surges.[1–4] Many 3C appliances nowadays are operated with rechargeable batteries. The voltage provided by the batteries is low. The multilayer varistors (MLV) are therefore developed for such low voltage applications. For multilayer components, the choice of inner electrode is important to their cost and performance. Previous study indicated that precious metal Pt is chemically inert to ZnO–Bi_2O_3-based ceramic.[5] Metallic Pt can therefore be used as the inner electrode for MLV. Since the layer thickness is small in MLV, the growth of ZnO grains is constrained by the limited space available between the Pt inner electrodes.[5]

The cost of Pt is very high. The 70%Ag–30%Pd alloy is now considered as the material for inner electrode. The basic requirement on inner electrode is its ability to co-fire with ZnO-based ceramics in air at elevated temperatures. For low voltage applications, the layer thickness between inner electrodes has to be small. The grain growth behaviour within a small space is not the same as that in the bulk specimen.[5,6] For example, the grain growth behaviour in multilayer specimen[5] and in thin film[6] is different from that in a bulk specimen. Furthermore, previous studies indicated that Bi_2O_3 could react with Pd at elevated temperatures.[7,8] Such reaction may affect the grain growth behaviour within the inner electrodes. However, the grain growth behaviour within AgPd inner electrodes has not been investigated before. In the present study, the grain growth behaviour of Bi_2O_3-doped ZnO grains within AgPd inner electrodes is thus investigated.

2. Experimental

A high-purity ZnO and 5 wt% Bi_2O_3 were mixed with solvents and binders first. The tape with a thickness of 20 μm was then prepared by tape casting. The AgPd (70%Ag–30%Pd) paste was deposited onto the green tape by screen printing. Laminating different numbers of green tapes made a multilayer structure with various thicknesses from 20 to 140 μm. To facilitate the comparison, the layers with different thickness were all built into one component. The schematics of the electrode configuration are shown in Fig. 1. The laminates were then cut into a size of 1.85 mm (length) × 0.95 mm (width) × 0.75 mm (thickness). All specimens were firstly fired from room temperature to 400 °C in air for 1 h using a heating rate of 1 °C/min to remove the organics. After the binder burnout stage, the sintering was performed in air at 900–1100 °C for various times. Several bulk specimens with the same composition were also prepared for comparison purpose. The thickness of the bulk specimens was around 3 mm. In order to prevent the evaporation of Bi_2O_3 during sintering, the specimens were sintered in a powder bed which composition was the same as that of the specimens.[9]

In order to carry out the microstructure analysis, the specimens were ground with SiC abrasive papers and polished with 0.05 μm Al_2O_3 particles. The specimens were etched with

* Corresponding author. Tel.: +886 2 33663899.
E-mail address: tuan@ntu.edu.tw (W.-H. Tuan).

0955-2219/$ – see front matter © 2009 Elsevier Ltd. All rights reserved.
doi:10.1016/j.jeurceramsoc.2009.05.008

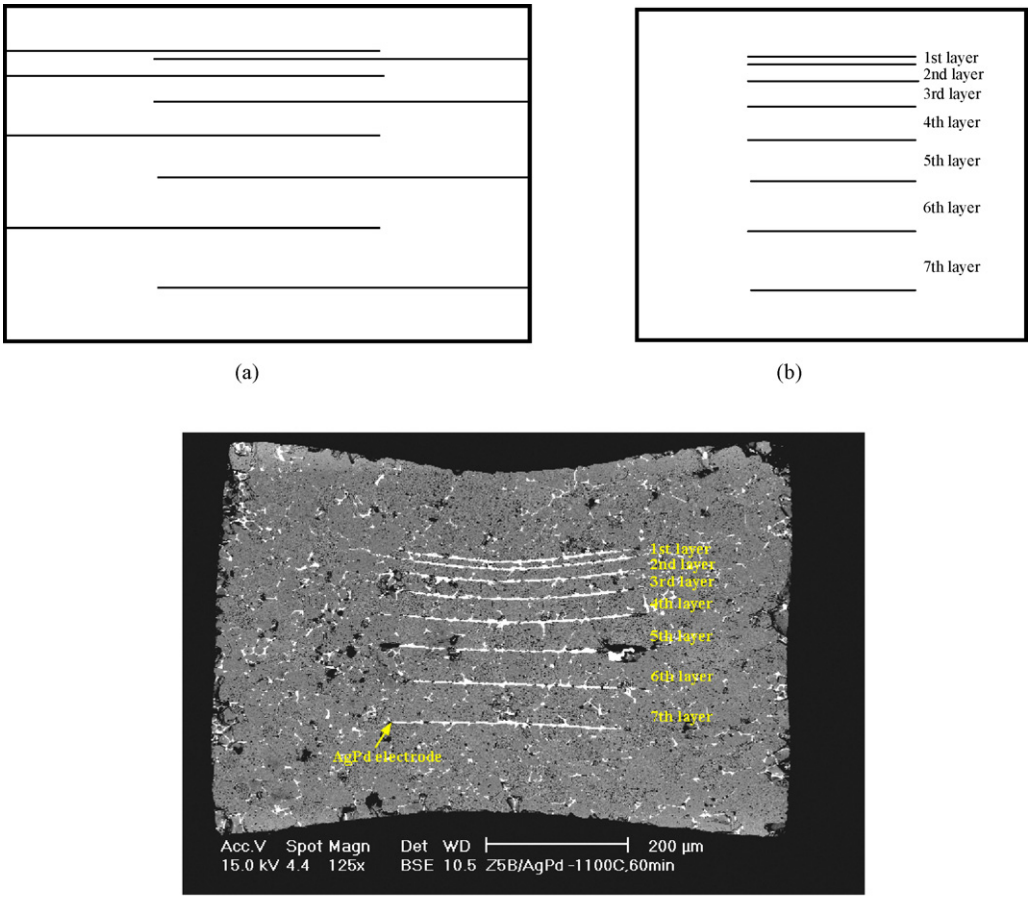

Fig. 1. (a) Side view and (b) cross-section for the electrode configuration of an MLV. (c) Cross-section of a typical ZnO–Bi_2O_3/AgPd MLV specimen after sintering at 1100 °C for 60 min.

dilute hydrochloric acid. The microstructures were observed by using scanning electron microscopy (SEM, XL-30, Philips Co., Netherlands). The size of ZnO grains was determined by applying an image analysis technique.[5] By assuming that each grain is spherical in shape, the size of ZnO grains was estimated. The composition analyses were carried out by using electron probe micro-analyzer (EPMA, Model JAX-8200, JOEL, Japan). Phase analysis of the sintered specimens was characterized with a synchrotron X-ray source (Beam-line 17B1, National Synchrotron Radiation Research Center, Hsinchu, Taiwan). Before the phase analysis, several multilayer specimens were mounted together into resin then ground to expose the cross-sections. The synchrotron X-ray beam was then spotted at the cross-sections of the specimens to carry out the phase analysis.

3. Results

Fig. 1(c) shows the cross-section of one typical MLV specimen after sintering at 1100 °C for 60 min. There are seven ceramic layers in the MLV specimen. The layer thickness varies from 8 to 55 μm after sintering. The volume shrinkage at the middle of the MLV specimen is larger than that at the two ends. Fig. 2 shows the XRD pattern of the MLV specimens after

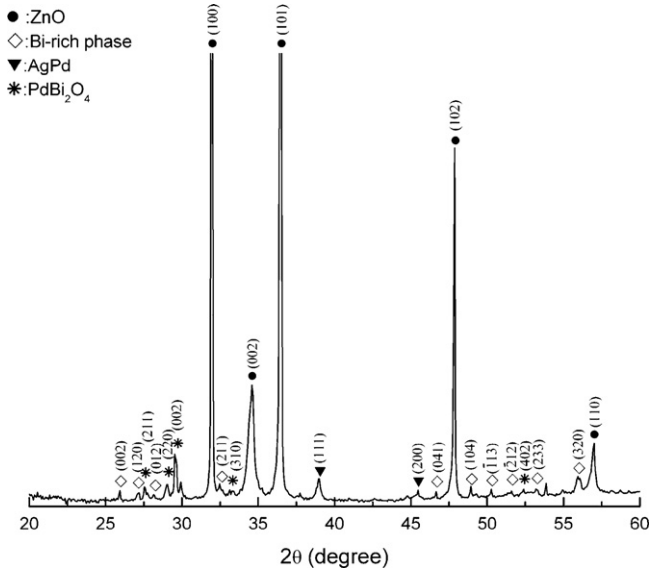

Fig. 2. XRD pattern of the ZnO–Bi_2O_3/AgPd MLV specimen after sintering at 1100 °C for 60 min.

sintering at 1100 °C for 60 min. Apart from ZnO, Bi_2O_3-rich phase and AgPd alloy, a reaction phase $PdBi_2O_4$ is also found. However, the intensity of the newly formed $PdBi_2O_4$ phase is relatively small.

The typical micrographs of the bulk and MLV specimens are shown in Fig. 3. Since the layers with various thicknesses

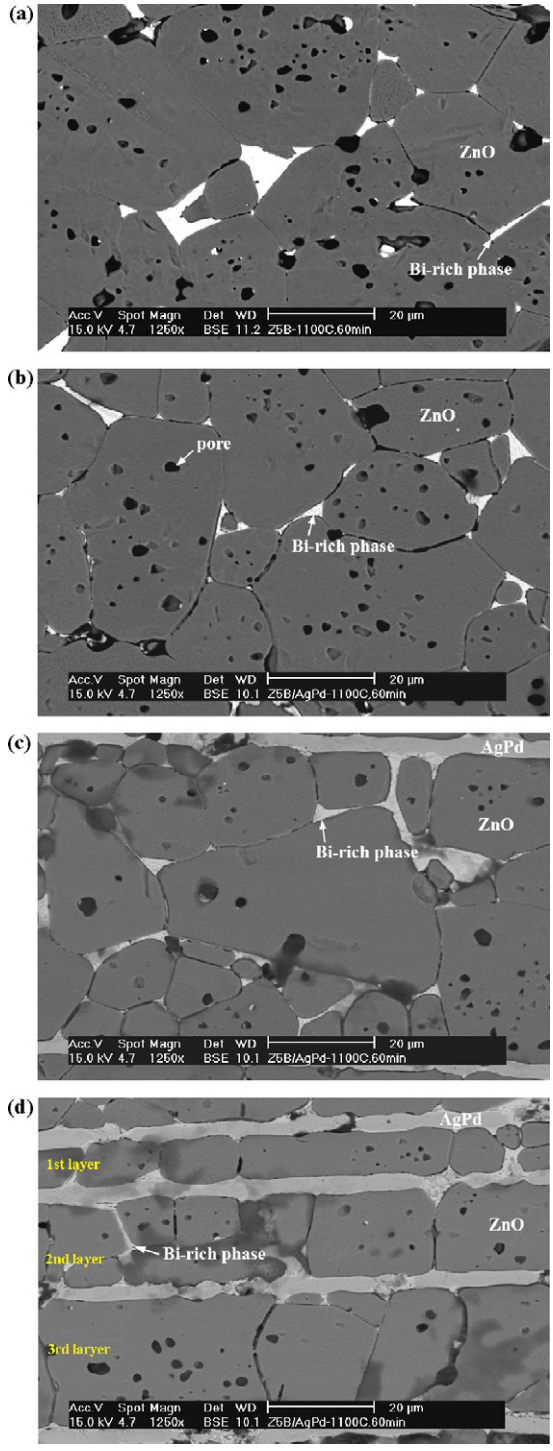

Fig. 3. Typical SEM micrographs of the (a) bulk and (b–d) MLV specimens. Micrographs show the microstructures (b) outside the AgPd inner electrodes and within the (c) 7th and (d) 1st to 3rd layers. The specimens were sintered at 1100 °C for 60 min.

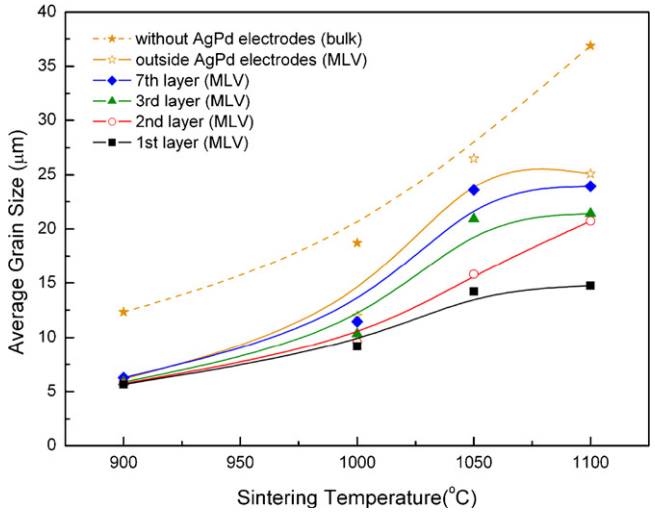

Fig. 4. Average size of ZnO grains in the bulk and MLV specimens after sintering at the indicated temperatures for 60 min.

are next to each other, the effect of the layer thickness on the grain growth behaviour can be estimated. Large grains with size >20 μm can be found in the bulk specimen, Fig. 3(a). Such large grains are also found in the area outside the inner electrodes, Fig. 3(b), and in the thick layer, Fig. 3(c). However, no such large grains are found in the thin layers, Fig. 3(d). Instead, some columnar grains are found in the thin layers.

The size of ZnO grains in the MLV and bulk specimens as a function of sintering temperature is shown in Fig. 4. The size of ZnO grains in the MLV specimen is smaller than that in the bulk specimens. For the MLV specimen, as the sintering temperature is 900 °C, the grain size within inner electrodes is the same as that outside the electrodes. With the increase of sintering temperature, the size of ZnO grains then decreases with the decrease of the layer thickness. Fig. 5 shows the size variation of the ZnO grains in the bulk and MLV specimens. Though the average size of the grains outside the inner electrodes is smaller than that in the bulk specimen, Fig. 4, the size variation of the

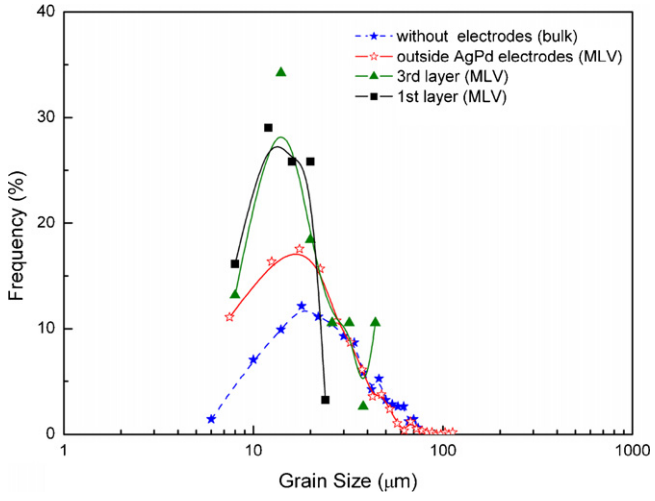

Fig. 5. Size distribution of the ZnO grains in bulk and MLV specimens after sintering at 1100 °C for 60 min.

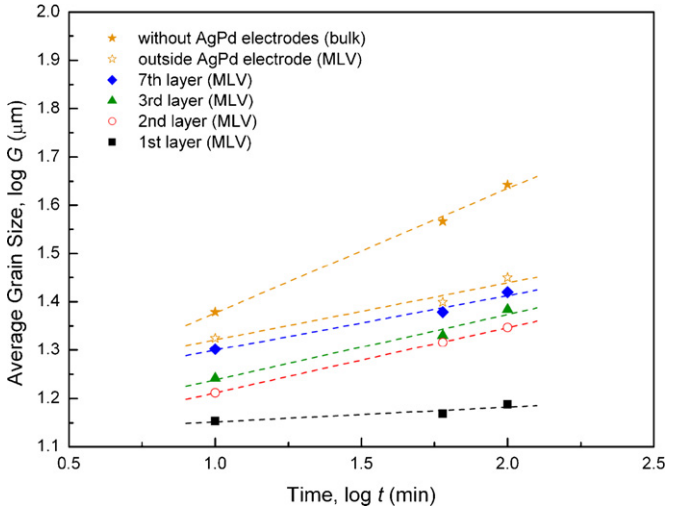

Fig. 6. Average size of ZnO grains in bulk and MLV specimens as a function of dwell time at 1100 °C.

grains outside the inner electrodes is very similar to that in the bulk specimen. However, the size scatter of the grains within the inner electrodes is smaller than that outside the electrodes.

Fig. 6 shows the size of ZnO grains as a function of dwell time at 1100 °C. The grain growth exponents for the various places within MLV specimens are shown in Table 1. Since the growth of the grains in the 1st layer is very limited, its grain growth kinetic constant is not calculated. By knowing the grain growth exponents (n), the apparent activation energy (Q) for the growth of ZnO grains can then be calculated. The values for the activation energy are also shown in Table 1. The n and Q values for the growth of ZnO grains in the MLV specimen are significantly higher than those in the bulk specimen. It indicates that the grain growth kinetics of the grains in MLV specimens are very much different from those in bulk specimens.

4. Discussion

A novel laminated structure is used in the present study. Seven layers with various thicknesses are incorporated into one laminated structure. Such structure allows us to look into the grain growth behaviour within a multilayer specimen. The cross-section of a green MLV specimen is rectangular in shape before sintering. The shape distortion of MLV specimens is noted after sintering, Fig. 1. The shrinkage is larger in the middle part of the MLV specimen. From Fig. 3, the amount of pores and their size in the thinner layers in the MLV specimen are smaller than those in the bulk specimens. A small amount of Ag can dissolve into ZnO at elevated temperature.[10] Since the Ag solute can enhance the grain growth rate of ZnO[10]; it may also enhance the densification of ZnO, also due to that the grain size decreases with the decrease of the layer thickness, the densification thus increases with the decrease of layer thickness.

Table 1
Calculated grain growth exponent (n) and apparent activation energy (Q) for the ZnO–Bi_2O_3 bulk and ZnO–Bi_2O_3/AgPd MLV specimens.

	Grain growth exponent, n	Apparent activation energy, Q/kJ/mol
Bulk	4	285
MLV		
Outside electrodes	9	931
7th layer	9	872
3rd layer	7	655
2nd layer	7	610
1st layer	–[a]	–[a]

[a] See text.

The ZnO grains outside the AgPd inner electrodes are smaller than those in the bulk specimens, see Fig. 4. Furthermore, the size of ZnO grains decreases with the decrease of layer thickness, indicating that the growth of the ZnO grains is constrained by the space available for them to grow. A powder bed is used in the present study, the Bi_2O_3-rich liquid phase remains after sintering, see Fig. 3. The Bi_2O_3-rich liquid phase can react with Pd to form $PdBi_2O_4$, Fig. 2. A very small amount of $PdBi_2O_4$ phase is thus found. Since the amount of the $PdBi_2O_4$ phase is small and the phase is likely formed during the cooling down stage,[8] the presence of the reaction phase affects little on the growth of ZnO grains.

For the bulk specimens, the grain growth kinetic constants, grain growth exponent and activation energy, are close to the reported values in the previous studies.[11,12] Dye and Bradt suggested that the growth of ZnO grains is controlled by the diffusion through the Bi_2O_3-rich liquid phase.[12] In the beginning of sintering, the size of the ZnO grains within the electrodes is the same as that outside the electrodes. As the size of ZnO grains approaching the layer thickness, the inner electrodes act as the diffusion barrier to the mass transportation. The growth in the direction perpendicular to the electrode is no longer possible. The size of ZnO grains is therefore small within the inner electrodes. Since the ZnO grain can grow only in the direction parallel to the direction of the inner electrodes and the Bi_2O_3-rich phase tends to perpendicular to the inner electrodes to decrease its length; columnar grains are thus formed in the 1st, 2nd and 3rd layers, see Fig. 3(d).

In the present study, an image analysis technique is used to determine the area of each grain. The area is then transferred into the grain size by assuming that the grain is spherical in size. As the columnar grain is formed, the calculated grains size is larger than the thickness of 1st layer (see Fig. 5). In fact, the width of the columnar grains is never larger than their layer thickness.

As far as the grain growth kinetic is concerned, the growth of grains depends on the number of routes for mass transportation. Since the grain growth can be seen as the movement of grain boundary as[6,13]:

$$v = \beta MF \quad (1)$$

where v is the velocity of the grain boundary movement, β is the geometric factor which depends on the routes available for the mass flow, F is the force and M is the intrinsic mobility of the boundary. The liquid remains throughout the sintering due to the use of a powder bed.[5] At the beginning of sintering, the available routes for mass transportation at different locations within a

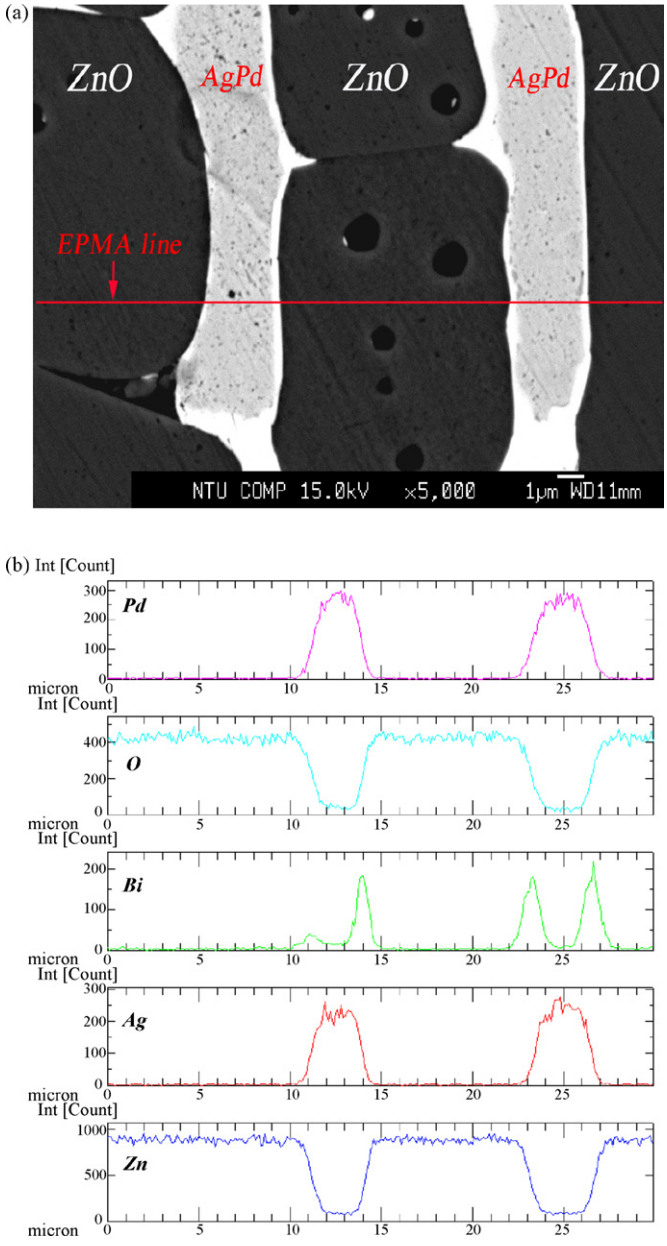

Fig. 7. (a) SEM micrograph of the 1st in MLV specimen after sintering at 1100 °C for 100 min, and (b) the corresponding EPMA line analysis.

multilayer structure are the same. The size of grains shows little dependence on the locations at the beginning of sintering, Fig. 4. However, the available mass transportation paths decrease when the ZnO grains touch the upper and bottom electrodes. It results in the reduction of the value of β (Eq. (1)). The growth of the ZnO grains within inner electrode is thus prohibited as they touch the inner electrodes. Since the Bi_2O_2-rich liquid phase remains between ZnO grains throughout the sintering stage, the grain growth mechanism is controlled by the diffusion through the liquid phase. Though the grain growth kinetic constants, grain growth exponent and activation energy, vary with the locations within the multilayer structure (Table 1), it reflects only the fact that the mass transportation paths decrease with the decrease of layer thickness.

The EPMA analysis indicates that there is a Bi_2O_3-rich liquid phase present between ZnO grain and AgPd electrode, Fig. 7(b). Furthermore, the Bi_2O_3-rich liquid phase seems to wet the AgPd electrode well, as demonstrated in Fig. 7(a). Since the Bi_2O_2-rich liquid phase is an electrical insulating layer, its presence establishes an electrostatic barrier at ZnO/ZnO grain boundary. Similarly, its presence at the ZnO/AgPd interface may also plays an important on the electrical properties of MLV. Detailed investigation into the ZnO/Bi_2O_3/AgPd boundary layer is needed.

5. Conclusions

Through careful microstructure characterization, the following remarks on the grain growth behaviour within ZnO–Bi_2O_3/AgPd multilayer varistors can be made.

(1) At the beginning of sintering, the size of ZnO grains is similar at different locations within the laminated structure.
(2) As the size of grains approaching the layer thickness, the grain boundaries tend to perpendicular to the electrodes. Columnar grains are thus formed.
(3) The average size of ZnO grains decreases with the decrease of layer thickness.
(4) The extent of size variation also decreases with decreasing layer thickness.
(5) The wetting of Bi_2O_3-rich liquid phase on AgPd electrode is taken place during co-firing.

Acknowledgments

The present study was supported by the National Science Council, Taiwan through the contract number of NSC94-2216-E-002-014. The technical help from Huey-Ru Chen, Walsin Technology Corporation, Kaohsiung, Taiwan, is highly appreciated.

References

1. Levinsion, L. M. and Philipp, H. R., Zinc oxide varistors—a review. *Am. Ceram. Soc. Bull.*, 1986, **65**(4), 639–649.
2. Gupta, T. K., Application of zinc oxide varistors. *J. Am. Ceram. Soc.*, 1990, **73**(7), 1817–2177.
3. Clarke, D. R., Varistor ceramics. *J. Am. Ceram. Soc.*, 1999, **82**(3), 485–502.
4. Cai, J., Lin, Y. H., Li, M., Nan, C. W., He, J. and Yuan, F., Sintering temperature dependence of grain boundary resistivity in a rare-earth-doped ZnO varistor. *J. Am. Ceram. Soc.*, 2007, **90**(1), 291–294.
5. Kuo, S. T., Tuan, W. H., Lao, Y. W., Wen, C. K. and Chen, H. R., Grain growth behavior of Bi_2O_3-doped ZnO grains in a multilayer varistor. *J. Am. Ceram. Soc.*, 2008, **91**(5), 1572–1579.
6. Thompson, C. V., Grain growth in thin film. *Annu. Rev. Mater. Sci.*, 1990, **20**, 245–268.
7. Wang, S. F. and Huebner, W., Interaction of silver/palladium electrodes with lead- and bismuth-based electroceramics. *J. Am. Ceram. Soc.*, 1993, **76**(2), 474–480.
8. Kuo, S. T., Tuan, W. H., Lao, Y. W., Wen, C. K., Chen, H. R. and Lee, H. Y., Investigation into the interactions between Bi_2O_3-doped ZnO and AgPd electrode. *J. Eur. Ceram. Soc.*, 2008, **28**, 2557–2562.
9. Lao, Y. W., Kuo, S. T. and Tuan, W. H., Effect of powder bed on the microstructure and electrical properties of Bi_2O_3- and Sb_2O_3-doped ZnO. *J. Mater. Sci. Mater. Electron.*, 2009, **20**, 234–241.

10. Kuo, S. T., Tuan, W. H., Shieh, J. and Wang, S. F., Effect of Ag on the microstructure and electrical properties of ZnO. *J. Eur. Ceram. Soc.*, 2007, **27**, 4521–4527.
11. Senda, T. and Bradt, R. C., Grain growth in sintered ZnO and ZnO–Bi_2O_3 ceramics. *J. Am. Ceram. Soc.*, 1990, **73**(1), 106–114.
12. Dey, D. and Bradt, R. C., Grain growth of ZnO during Bi_2O_3 liquid-phase sintering. *J. Am. Ceram. Soc.*, 1992, **75**(9), 2529–2534.
13. Brook, R. J., *Controlled grain growth In Treatise on Materials Science and Technology*, *vol. 9*. Academic Press Inc., New York, 1976, p. 331.